

Air Charge Estimation for Turbocharged Diesel Engines

Ove F. Storset, Anna Stefanopoulou and Roy Smith
UC Santa Barbara, CA 93106

Abstract

The paper presents adaptive observers for in-cylinder air charge estimation for turbocharged diesel engines based on a mean value engine model. We assess the observability of various engine measurements. The performance of the observers is compared to existing schemes analytically and in simulations. Specifically, it is shown that the designed observers perform better than the conventional schemes during fast step changes in engine fueling level. Furthermore, the estimate is less sensitive to changes in engine parameters than the existing schemes.

1 Introduction and background

Fuel economy benefits obtained by turbocharged diesel engines render them common practice for the vast majority of medium and heavy duty vehicles and are often met in passenger vehicles. Reduction of smoke emission, particulates, and oxides of nitrogen are challenges that need to be addressed by the vehicle controller to make the diesel-based propulsion more wide-spread. Diesel engines operate with a lean mixture of air and fuel. Visible smoke and particulates are generated when the air-to-fuel ratio decreases below a critical value. To maintain the air-to-fuel ratio above the visible smoke limit, the vehicle controller estimates the cylinder air charge and limits the amount of fuel injected in the cylinders. The estimation task here is more challenging than in gasoline engine due to the interaction of the intake, turbocharger and exhaust manifold dynamics. Furthermore, lean air fuel ratio is more difficult to measure in the tailpipe than the stoichiometric air fuel ratio typically met in gasoline engines [1]. Last, but not least, air charge estimation is very difficult during large exhaust gas recirculation (EGR) introduced to reduce NOx [2][3].

In this paper we address the air charge estimation problem without EGR, using adaptive observers. The observers provide better estimates during fueling transients than existing schemes, and the presented approach is less sensitive to modeling errors and aging than conventional schemes.

1.1 Notation

In the sequel $\bar{(\cdot)}$ denotes a measured variable, or a variable constructed from measurements only. Mass flows will have two indices, W_{kl} , where 'k' represents the origin of the flow and 'l' is the destination. Masses are denoted with m , and temperatures with T . The following indices are used: 'c' represents the compressor outlet, 'ic' is the intercooler outlet, '1' is the intake manifold, 'a' is ambient conditions, 'e' is the engine, and 'f' is fuel. \mathbb{R}_+ is the set of positive real numbers excluding zero; \dot{x} denotes $\frac{d}{dt}x$, and $\mathcal{P}^n(x)$ is a n -th order

polynomial in x .

2 Mean value model

The intake manifold dynamics are approximated using mean value modelling which disregards the engine events and the inertia of the gas. The flow through the engine is then continuous, and transportation delays are neglected (see Figure 1). This model is clearly not valid for short

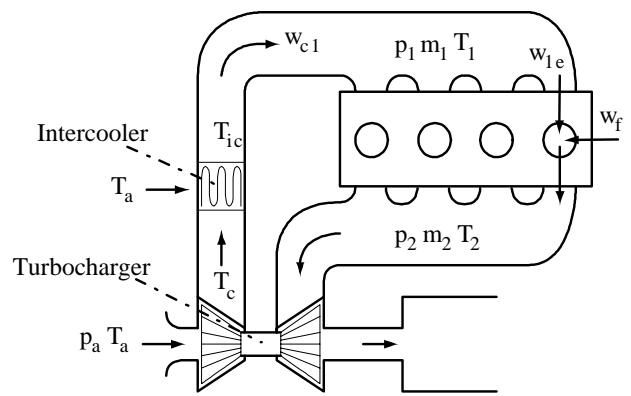


Figure 1: A turbo charged diesel engine with intercooler

time intervals, but it has a good accuracy down to one engine cycle [4]. The energy (1) and mass (2) balance of the intake manifold give equations for pressure, p_1 , and mass, m_1 , respectively. They are related by the intake manifold temperature, T_1 , through the ideal gas law (3).

$$\dot{p}_1 = \gamma k_1^2 (W_{c1} T_{ic} - W_{1e} T_1) \quad (1)$$

$$\dot{m}_1 = W_{c1} - W_{1e} \quad (2)$$

$$T_1 = \frac{1}{k_1^2} \frac{p_1}{m_1}, \quad k_1 = \sqrt{\frac{R_1}{V_1}} \quad (3)$$

where V_1 is the volume of the intake manifold, γ is the ratio of specific heats, and R_1 is the gas constant for air which is assumed constant. Heat dissipation has been ignored. Note that the intercooler temperature, T_{ic} , varies with compressor and intercooler efficiencies, thus equation (1) and (2) have a time-varying dependency. This time-varying dependency is usually neglected in conventional estimation schemes where T_{ic} and T_1 are assumed equal and constant.

The flow into a four cylinder engine, W_{1e} , is given by

$$W_{1e} = k_1^2 k_3 N m_1 \eta_v, \quad k_3 = \frac{V_d}{R_1 120}, \quad (4)$$

where V_d is the engine's total displacement volume. The volumetric efficiency, η_v , is typically in the range $\eta_v \in [\frac{1}{2}, 1]$. Intuitively, it is the averaged fraction of cylinder mass density to mass density in the intake manifold, where the averaging is taken over one engine cycle. More precisely,

$$\eta_v(t) = \frac{\frac{1}{V_d} \int_{t-\delta}^t W'_{1e}(\tau) d\tau}{\frac{1}{V_1} \frac{1}{T} \int_{t-\delta}^t m_1(\tau) d\tau}, \quad \delta = 2\frac{60}{N}, \quad (5)$$

where W'_{1e} is the instantaneous flow into the engine, whereas W_{1e} is the averaged quantity. η_v accounts for the filling and emptying dynamics of the cylinder which depend on engine speed, N ; temperature and pressure in the intake and exhaust manifolds, T_1, p_1, T_2, p_2 ; and the physical cylinder flow constraints. Since these phenomena are governed by complicated air flow patterns, it is difficult to give a precise analytic expression for η_v . Nevertheless, the volumetric efficiency is important for the dynamic behavior of W_{1e} . Note that in steady state the mean value flow into the engine equals the flow into the intake manifold, W_{c1} . We will assume that $\eta_v(t) \in \mathcal{S}_\eta := \{\eta_v | \eta_{vMIN} \leq \eta_v \leq \eta_{vMAX}\} \forall t \geq t_0$. A model for η_v that captures its dominant features is

$$\eta_v(t) = \mathcal{P}(N(t))\theta(t), \quad (6)$$

where $\mathcal{P}(N) > 0$ is a polynomial in N that accounts for the pumping rate's dependency on engine speed. $\theta(t) \in \mathcal{S}_\theta(t) := \{\theta | \mathcal{P}(N(t))\theta \in \mathcal{S}_\eta\} \subset \mathcal{S}_\theta \subset \mathbb{R}_+, \forall t \geq t_0$, and θ is an unknown coefficient that accounts for the other phenomena mentioned.

The model's state, $x^T := [p_1, m_1]$, is for physical reasons upper and lower bounded so that $x \in \mathcal{D} \subset \mathbb{R}_+^2$ where \mathcal{D} is compact. Since T_1 is related to p_1 and m_1 through (3) we can also assume $T_1 \in \mathcal{T}_1 \subset \mathbb{R}_+$, \mathcal{T}_1 compact. The input to the model is defined as $u^T := [W_{c1}, T_{ic}, N] \in \mathcal{U}$ where \mathcal{U} is compact. $\mathcal{U} \in \mathbb{R}_+^3$ under the assumption that there are no compressor surges.

2.1 Measurements

Sensor selection in engines depends on their cost, reliability and precision. The engine speed N is assumed measured throughout the sequel, and it is precise so we assume $\bar{N} = N$.

The flow into the intake manifold, W_{c1} , is typically measured with an air velocity sensor, but its performance deteriorates with use even for more expensive devices.

Intake manifold pressure, p_1 , can be measured precisely with a large bandwidth at moderate cost relative to W_{c1} . However, the engine events cause pressure fluctuations so that $\bar{p}_1 = p_1 + \Delta p_1$, where Δp_1 represents the higher order dynamics which are not present in the mean value model. Δp_1 typically has a rectified sinusoidal shape with frequency of the sinusoid equal to $2\pi N/60$ rad/s. These higher order dynamics appear as measurement "noise", and might destabilize the identified parameter $\hat{\eta}_v$.

Temperature measurements are typically done with thermocouples which have a time constant varying with the flow of air. The fastest thermocouples are significantly slower than p_1 measurements, so temperature measurements limit the observer bandwidth.

The intercooler air temperature, T_{ic} , can be constructed from other measurement with moderate accuracy as explained in Section 5. For better precision a measurement has to be taken, and the cost precision considerations are the same as for T_1 .

2.2 Traditional air charge estimation

In throttled spark ignited engines air charge estimation is traditionally achieved based on the measurement of intake manifold air flow using a map of the engine's steady state pumping rate $\mathcal{P}(N, p_1)$ as a replacement for W_{1e} . The temperature of air entering the intake manifold is assumed equal to T_1 , and \hat{p}_1 is estimated in an open loop observer as,

$$\dot{\hat{p}}_1 = \gamma k_1^2 T_1 (-\mathcal{P}(N, \hat{p}_1) + \bar{W}_{c1}) \quad (7)$$

$$\hat{W}_{1e} = \mathcal{P}(N, \hat{p}_1), \quad (8)$$

where T_1 is assumed constant or measured with a low bandwidth device [5]. In steady state the error $\tilde{W}_{1e} := W_{1e} - \hat{W}_{1e}$ is given by $\tilde{W}_{1e} = \tilde{W}_{c1}$ which is small when the measurement error $\tilde{W}_{c1} := W_{c1} - \bar{W}_{c1}$ is small; however, this is not always the case.

Another traditional air charge estimation algorithm is the so called speed density scheme. It utilizes a map of the steady state pumping rate, $\mathcal{P}(N, p_1)$, as a replacement for η_v ; T_1 is assumed constant, and p_1 is measured. In this scheme $W_{1e} = k_1^2 k_3 N m_1 \eta_v = k_3 N \frac{p_1}{T_1} \eta_v$ is approximated as $\hat{W}_{1e} \approx \mathcal{P}(N, \bar{p}_1)$. The speed density scheme relies even more on the accuracy of the $\mathcal{P}(N, p_1)$ map which accuracy might deteriorate as the engine ages.

Both schemes can be quite precise on large time scales in throttled gasoline engines if the map $\mathcal{P}(N, p_1)$ is an accurate representation of the steady state pumping rate. However, in diesel engines torque is controlled by varying the fueling level, whereas spark ignited engines uses cylinder air charge for this purpose. Consequently, in diesel engines, the fueling level and possibly the opening of the variable geometry turbine affects p_2 very rapidly, and p_2/p_1 varies significantly during transients as shown in Figure 3 [6]. In addition, for turbocharged engines, η_v is higher, and the filling and emptying dynamics are more sensitive to changes in p_2 and p_1 which in turn causes η_v to have a transient characterization different from its steady state behavior. The parameterization $\eta_v(N, p_1)$ does not account for this behavior. One could develop a more precise parameterization of η_v as in [6] [7]; however, this requires a p_2 measurement which is not desirable due to the harsh conditions in the exhaust manifold, and avoid visible smoke emissions.

Since neither of the traditional schemes accounts for the dynamic properties of η_v , there is a significant error in the estimate when the fueling level changes which alters the volumetric efficiency. Unfortunately, this is exactly when a reliable air charge estimate is needed to maintain an acceptable air to fuel ratio.

3 Proposed solution

To estimate the air charge, W_{1e} , more precisely we need to have more information about the variations in η_v in addition to a satisfactory \hat{m}_1 estimate. We seek to obtain this by parameterizing the volumetric efficiency by $\eta_v(t) = \mathcal{P}(N(t))\theta(t)$ and attempt to identify the unknown coefficient $\theta(t)$ through an identification scheme relying on variables estimated by an observer. We will present the fol-

lowing schemes:

scheme	measurements	m_1 estimate
1	p_1, W_{c1}, N, T_a	open loop
2	p_1, T_1, N, T_{ic}	closed loop

It is advantageous to have a closed loop observer since it will reduce the observer's sensitivity to modelling and input measurement errors and increase the convergence rate of the estimates. This is only possible if observability is achieved by the correct choice of measurements, and additional conditions are satisfied. Notice that even if a perfect model is obtained, an error in the measurements due to the structure of the equations (1)-(3) will create a bias in the identified parameter, $\theta(t)$, which we seek to avoid.

4 Observability of the model

We start with a few remarks on nonlinear observability, and the challenges in nonlinear observer design. If we assume that we have perfect knowledge of the plant, the inputs and the outputs except its present state, the issue of observability addresses whether it is possible to create an observer whose state estimate converges faster to the actual state than the plants dynamics. Observability for nonlinear systems is defined in terms of indistinguishable states [8]. However, for nonlinear systems, observability is in general not enough to be able to design a closed loop observer. The additional condition of the plant being uniformly observable (UO) guarantees the existence of an observer for the system.

To estimate \dot{W}_{1e} we need to produce an estimate of m_1 since it can not be measured directly. If the input, $u = [W_{c1}, T_{ic}, N]$, is known, observability of m_1 can then be assessed from p_1 and or T_1 measurements assuming correct system equations, (9)-(11), and perfect knowledge of $\eta_v = \mathcal{P}(N)\theta$.

Equations (1)-(3) can be written

$$\begin{bmatrix} \dot{p}_1 \\ \dot{m}_1 \end{bmatrix} = \begin{bmatrix} -\gamma k_1^2 k_3 N(t) \eta_v(t) p_1 + \gamma k_1^2 W_{c1} T_{ic} \\ -k_1^2 k_3 N(t) \eta_v(t) m_1 + W_{c1} \end{bmatrix} \quad (9)$$

$$T_1 = g_1(x) = \frac{1}{k_1^2} \frac{p_1}{m_1} \quad (10)$$

$$p_1 = g_2(x) = p_1 \quad (11)$$

where $x^T = [p_1, m_1]$ is the state.

If we consider $y = T_1$ the system is observable. Further analysis reveals that there are no non universal inputs in \mathcal{U} , so (9) is uniformly observable from (10) [9].

If we consider $y = p_1$ the output equation (11) does not contain m_1 , and since the system (9) is decoupled, all pairs of states $([p_1(t_0), m_1(t_0)]^T, [p_1(t_0), m'_1(t_0)]^T)$, $\forall m_1(t_0) \neq m'_1(t_0)$ are indistinguishable so the system is not observable.

If both p_1 and T_1 are measured the system (9)-(11) is obviously observable since it is so in the case when only T_1 is measured.

5 Approximation for intercooler temperature

Since the time constant of temperature measurements is typically large, T_{ic} must be constructed from available high

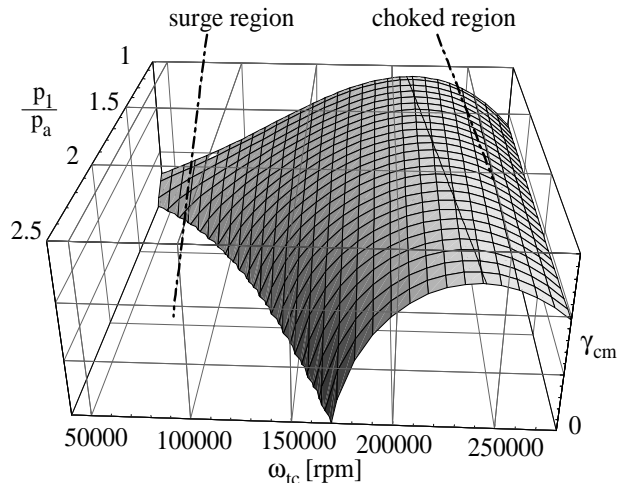


Figure 2: Typical curve fit of compressor mass flow parameter, γ_{cm} .

bandwidth measurements. We seek to obtain an approximation of T_{ic} based on measurements of p_1 and W_{c1} using available models of the turbocharger and intercooler.

The temperature out of the compressor is

$$T_c = T_a \left[1 + \frac{1}{\eta_c \left(\frac{p_1}{p_a}, \omega_{tc} \right)} \left(\left(\frac{p_1}{p_a} \right)^{\frac{\gamma-1}{\gamma}} - 1 \right) \right], \quad (12)$$

where T_a and p_a are ambient temperature and pressure respectively, and ω_{tc} is turbocharger speed. The compressor efficiency, $\eta_c(p_1, \omega_{tc})$, is the ratio of isentropic temperature rise to the actual temperature rise across the compressor, and is used to compensate for the losses caused by other physical effects which are difficult to model (see [10]). This model does not capture the heat storage effects of the compressor body, so the actual compressor temperature deviates slightly from this. If an intercooler with air coolant is used, the temperature out of the intercooler, T_{ic} , becomes

$$\begin{aligned} T_{ic} &= T_a \left[1 + \frac{1}{\eta_c \left(\frac{p_1}{p_a}, \omega_{tc} \right)} \left(\left(\frac{p_1}{p_a} \right)^{\frac{\gamma-1}{\gamma}} - 1 \right) (1 - \eta_{ic}) \right] \\ &= T_a \gamma_{T_{ic}} \left(\frac{p_1}{p_a}, \omega_{tc}, \eta_{ic} \right), \end{aligned} \quad (13)$$

where the intercooler efficiency, η_{ic} , can be treated as a constant or modelled as a function of the flow W_{c1} and/or vehicle speed v .

The flow through the compressor, W_{c1} , is typically modelled with a map, $\gamma_{cm} \left(\frac{p_1}{p_a}, \omega_{tc} \right)$, called the compressor mass flow parameter,

$$W_{c1}(p_1, \omega_{tc}, p_a, T_a) = \frac{p_a}{\sqrt{T_a}} \gamma_{cm} \left(\frac{p_1}{p_a}, \omega_{tc} \right), \quad (14)$$

and a typical shape of this map is given in Figure 2. If the operating point $\left(\frac{p_1}{p_a}, \omega_{tc} \right)$ is to the left of the surge line, the compressor flow is unstable which may cause reverse flow. If the compressor flow reaches the speed of sound, choking occurs; any further increase of ω_{tc} will not increase the flow. The steady state operating point $(p_1, \omega_{tc})_{ss}$ is determined by the steady state flow into the engine, the fueling level and VGT opening.

The maximum allowable intake manifold pressure limits the turbocharger speed, which in turn restricts the dynamic deviations of the steady state operating point, $(p_1, \omega_{tc})_{ss}$, away from the choking region. Surges can occur but only for short periods of time if we assume a reasonable controller. In this operating region the map $f_\gamma : (\frac{p_1}{p_a}, \omega_{tc}) \rightarrow \gamma_{cm}$ is one-to-one so that the function $f_\omega : (\frac{p_1}{p_a}, \gamma_{cm}) \rightarrow \omega_{tc}$ is well defined, and the compressor speed can be modeled as a function of the measurements p_1 and W_{c1} as

$$\omega_{tc} = f_\omega\left(\frac{p_1}{p_a}, \gamma_{cm}\right) = f_\omega\left(\frac{p_1}{p_a}, \frac{\sqrt{T_a}}{p_a} W_{c1}\right).$$

If we insert this expression into η_c we get.

$$\eta_c = \eta_c\left(\frac{p_1}{p_a}, \omega_{tc}\right) = \eta_c\left(\frac{p_1}{p_a}, f_\omega\left(\frac{p_1}{p_a}, \frac{\sqrt{T_a}}{p_a} W_{c1}\right)\right),$$

and construct the compressor efficiency based on measurements of p_1, W_{c1}, p_a, T_a

$$\hat{\eta}_c = \eta_c(\bar{p}_1, \bar{W}_{c1}, \bar{p}_a, \bar{T}_a).$$

\bar{T}_{ic} then becomes

$$\begin{aligned} \bar{T}_{ic} &= \bar{T}_a \left[1 + \frac{1}{\hat{\eta}_c(\bar{p}_1, \bar{W}_{c1}, \bar{p}_a, \bar{T}_a)} \left(\left(\frac{\bar{p}_1}{\bar{p}_a} \right)^{\frac{\gamma-1}{\gamma}} - 1 \right) \times \right. \\ &\quad \left. (1 - \eta_{ic}) \right] = \bar{T}_a \bar{\gamma}_{T_{ic}} \left(\frac{\bar{p}_1}{\bar{p}_a}, \bar{W}_{c1}, \eta_{ic} \right), \end{aligned} \quad (15)$$

where p_a and T_a can be measured with a low bandwidth devices or assumed constant.

Since the compressor efficiency, η_c , varies little along the steady state operating point $(\frac{p_1}{p_a}, \omega_{tc})_{ss}$ it can be treated as a constant. Then, $\bar{\gamma}_{T_{ic}}$ becomes a function of only the pressure ratio across the compressor and the intercooler efficiency $\bar{\gamma}_{T_{ic}}(\frac{p_1}{p_a}, \eta_{ic})$. This is acceptable for $(\frac{p_1}{p_a}, \omega_{tc})_{ss}$ close to steady state, but transient deviations cause perturbations in η_c especially for $(\frac{p_1}{p_a}, \omega_{tc})$ close to the surge line.

These approximations suffer from the general uncertainty in modelling compressor behavior, and should be considered only as the best currently available alternative to treating T_{ic} constant or equal to T_1 .

6 Observer Scheme 1

We will first assume that only \bar{p}_1 and \bar{W}_{c1} are measured with possible errors, that $\bar{N} = N$, and that \bar{T}_{ic} is constructed from p_1 and a slow T_a measurement (see section 5). We will pursue the estimation of W_{1e} by identifying the unknown parameter $\theta(t)$. Since m_1 is unobservable from the measurements it is not possible to make a closed loop observer of m_1 , so we use the open loop observer

$$\dot{\hat{m}}_1 = -k_1^2 k_3 N \hat{m}_1 \mathcal{P}(N) \hat{\theta} + \bar{W}_{c1} \quad (16)$$

$$\dot{\hat{W}}_{1e} = k_1^2 k_3 N \mathcal{P}(N) \hat{m}_1 \hat{\theta}, \quad (17)$$

and we use the estimate of p_1

$$\begin{aligned} \dot{\hat{p}}_1 &= -\gamma k_1^2 k_3 N \bar{p}_1 \mathcal{P}(N) \hat{\theta} + \gamma k_1^2 \bar{W}_{c1} \bar{T}_{ic} \\ &\quad + g_{p1} (\bar{p}_1 - \hat{p}_1), \quad g_{p1} > 0 \end{aligned} \quad (18)$$

to create an identification error for the unknown parameter $\theta(t)$. To make a reliable identification scheme for θ we have to find a parameterization of (1) that is linear in θ to guarantee

convergence of $\hat{\eta}_v$ to η_v . Manipulating (1) and substituting the parameterization for η_v (6) gives

$$\begin{aligned} &\left(\frac{d}{dt} p_1 \right)(t) - \gamma k_1^2 W_{c1}(t) T_{ic}(t) \\ &= -\gamma k_1^2 k_3 N(t) p_1(t) \mathcal{P}(N(t)) \theta(t). \end{aligned}$$

Filtering both sides with the stable filter H_f yields

$$\begin{aligned} &\left[H_f \left(\frac{d}{dt} p_1 \right)(\tau) \right] (t) - \gamma k_1^2 (H_f W_{c1} T_{ic})(t) \\ &= -\gamma k_1^2 k_3 (H_f N \mathcal{P}(N) p_1 \theta)(t), \end{aligned}$$

and defining $(\phi\theta)(t) := -\gamma k_1^2 k_3 (H_f N \mathcal{P}(N) p_1 \theta)(t)$ and $(H_{df})(t) := (H_f \frac{d}{dt})(t)$ gives

$$z(t) := (H_{df} p_1)(t) - \gamma k_1^2 (H_f W_{c1} T_{ic})(t) = (\phi\theta)(t). \quad (19)$$

To implement this scheme we use the estimate \hat{p}_1 of p_1 to create $\hat{z} = \phi\hat{\theta}$. If we define $\tilde{p}_1 = p_1 - \hat{p}_1$ the identification error, $\epsilon = z - \hat{z}$, becomes:

$$\begin{aligned} \epsilon(t) &= (z - \hat{z})(t) = (H_{df} p_1)(t) - \gamma k_1^2 (H_f W_{c1} T_{ic})(t) \\ &\quad - [(H_{df} \hat{p}_1)(t) - \gamma k_1^2 (H_f \bar{W}_{c1} \bar{T}_{ic})(t) \\ &\quad + (H_f g_{p1} (p_1 - \hat{p}_1))(t)] \\ &= ((H_{df} + g_{p1} H_f) \tilde{p}_1)(t) - \gamma k_1^2 (H_f \widetilde{W_{c1} T_{ic}})(t) \quad (20) \\ &= (\phi\theta)(t) - (\phi\hat{\theta})(t) = \tilde{\theta}(t) \phi(t) + \epsilon_s, \end{aligned}$$

where $\widetilde{W_{c1} T_{ic}}(t) = W_{c1}(t) T_{ic}(t) - \bar{W}_{c1}(t) \bar{T}_{ic}(t)$ and ϵ_s is the swapping terms from pulling $\tilde{\theta}(t) = \theta(t) - \hat{\theta}(t)$ through the filter $(H_f)(t)$. Since there is no information about $\widetilde{W_{c1} T_{ic}}(t)$ available, this term is neglected, but it will cause a bias in the estimate $\hat{\theta}(t)$. To implement this identification scheme we have to use the measurement $\bar{p}_1(t) = p_1(t) + \Delta p_1(t)$. Since the frequency of the disturbance $\Delta p_1(t)$ is varying with $N(t)$ it is beneficial to make the cutoff frequency of the filters $(H_{df})(t)$ and $(H_f)(t)$ dependent on $N(t)$, and implement $\epsilon(t) = ((H_{df}(\tau) + g_{p1} H_f(\tau)) \tilde{p}_1)(t)$ as

$$\begin{aligned} \dot{x}_\epsilon &= -k_\omega N(t) x_\epsilon + k_\omega N(t) (g_{p1} - k_\omega N(t)) (\bar{p}_1 - \hat{p}_1) \\ \epsilon &= x_\epsilon + k_\omega N(t) (\bar{p}_1 - \hat{p}_1), \end{aligned} \quad (21)$$

and $\phi(N(t), t)$ as

$$\begin{aligned} \dot{x}_\phi &= -k_\omega N(t) x_\phi - k_\omega N(t) \gamma k_1^2 k_3 N p_1 \mathcal{P}(N) \\ \phi &= x_\phi. \end{aligned} \quad (22)$$

The updating law

$$\dot{\hat{\theta}}(t) = \begin{cases} (\Gamma + P) \phi(t) \epsilon(t) & \hat{\eta}_v = \mathcal{P}(N) \hat{\theta} \in \mathcal{S}_\eta \\ 0 & \hat{\eta}_v = \mathcal{P}(N) \hat{\theta} \notin \mathcal{S}_\eta, \end{cases} \quad (23)$$

is the combination of the traditional gradient and least squares with projection and covariance resetting. $\Gamma > 0$, and $P(t)$ is given by

$$\dot{P}(t) = \begin{cases} -P^2(t) \phi^2(t) & \hat{\eta}_v = \mathcal{P}(N) \hat{\theta} \in \mathcal{S}_\eta \\ 0 & \hat{\eta}_v = \mathcal{P}(N) \hat{\theta} \notin \mathcal{S}_\eta \end{cases}, \quad (24)$$

where $P(t)$ is reset to $P(t_\tau) > 0$ when the fueling level of the engine changes faster than some chosen threshold. This gives faster adaption when the volumetric efficiency is expected

to change, whereas the gradient algorithm assures a small identification error in $\hat{\eta}_v$ when it changes slowly. To assure that $\hat{\eta}_v \in \mathcal{S}_\eta$, the update law utilizes projection. Notice that the projection set $\mathcal{S}_\theta(t)$ varies as $\mathcal{P}(N(t))$ varies with time. See [11] for a monograph on on-line identification.

Define the following conditions:

Condition 1 $x \in \mathcal{D}$ and $u \in \mathcal{U} \forall t \geq t_0$ where \mathcal{D} and \mathcal{U} are compact.

Condition 2 $\Delta p_1 = 0$ and $\tilde{W}_{c1} = 0 \forall t \geq t_0$, and \tilde{T}_{ic} and θ are independent of time.

Condition 3 $\tilde{T}_{ic} = 0, \forall t \geq t_0$.

Proposition 1 *The given adaptive observer (16) - (18) with the identification error (20) utilizing the filter(21) and (22) with the combined least squares and gradient updating law (23) and (24) with parameter projection has the following properties:*

1. Condition 1 implies $\hat{\theta}, \hat{p}_1, \hat{m}_1 \in \mathcal{L}_\infty$ (all signals are bounded)
2. If further 2 is satisfied $\tilde{W}_{1e} \rightarrow 0$ exponentially as $t \rightarrow \infty$
3. If conditions 1-3 are satisfied we additionally have that $\hat{\theta}, \hat{\eta}_v \rightarrow 0$ exponentially as $t \rightarrow \infty$

For a proof, see [9]

6.1 Effect of measurement errors

The pressure fluctuations due to the engine events will be present in \bar{p}_1 as Δp_1 . With this disturbance the estimation error will not be zero, but $\tilde{W}_{1e} \in \delta(\Delta p_1)$ where $\delta(\Delta p_1)$ is some small neighborhood of the origin.

A constant \tilde{T}_{ic} will make $\hat{\eta}_v$ biased, but \tilde{m}_1 will also be nonzero and will counteract $\hat{\eta}_v$ in the output equation (17):

$$\tilde{\eta}_v = \eta_v \left(1 - \frac{\tilde{T}_{ic}}{T_{ic}} \right), \quad \tilde{m}_1 = \frac{W_{c1}}{k_1^2 k_3 N \eta_v} \left(\frac{T_{ic}}{\tilde{T}_{ic}} - 1 \right),$$

$$\tilde{W}_{1e} = 0.$$

However, a time varying \tilde{T}_{ic} can cause errors in \tilde{W}_{1e} as the time constant of (16), $k_1^2 k_3 N \mathcal{P}(N) \theta$ determines the rate which \tilde{m}_1 counteracts $\hat{\eta}_v$.

If $\tilde{W}_{c1} \neq 0$, $\hat{\theta}$ will be biased. This bias will in general result in a smaller error during transients than the traditional scheme in Section 2.2, but the steady state error is

$$\tilde{\eta}_v = \eta_v \left(1 - \frac{\tilde{W}_{c1}}{W_{c1}} \right), \quad \tilde{m}_1 = 0, \quad \tilde{W}_{1e} = \tilde{W}_{c1}, \quad (25)$$

which is the same as in (7).

6.2 Implementation issues

The adaptive gain from the least squares $P(t_r) = f(N, W_f)$ should be made a function of engine speed and fueling level to assure the same rate of convergence of $\hat{\theta}$ at all operating points of the engine. Otherwise, the adaption might be very slow at low N and W_f , and oscillatory at high values of N , and W_f . Increased value of the adaptive gain

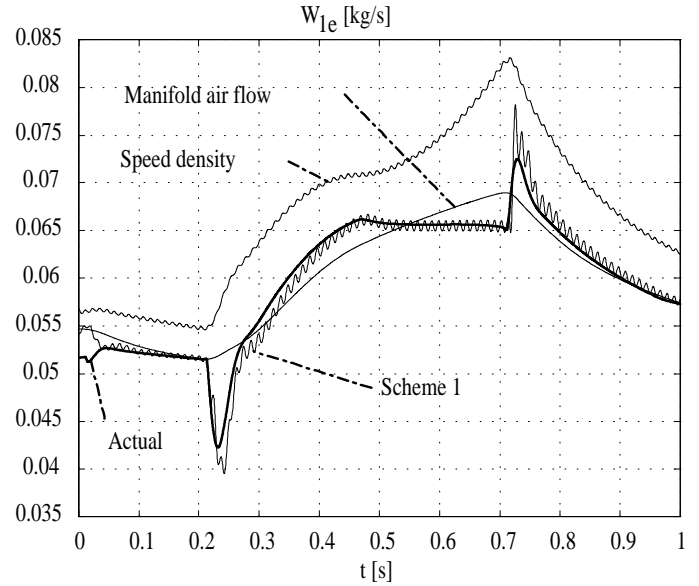


Figure 3: Air charge for scheme one, speed density and manifold air flow schemes

$\Gamma + P$ gives more measurement noise from \bar{p}_1 in $\hat{\theta}$. The filter coefficient k_w has a similar effect on the convergence of $\hat{\theta}$; set too high it creates more noise in $\hat{\theta}$, and too low results in slower convergence of $\hat{\theta}$.

The purpose of the feedback term, g_{p1} , in (18) is to prevent Δp_1 from destabilizing the adaptive scheme. Its purpose can heuristically be explained as making Δp_1 zero mean with respect to \hat{p}_1 . This way the error, $\bar{p}_1 - \hat{p}_1$, which drives the adaptive law, does not contain a constant component from the disturbance Δp_1 . Such constant disturbances can, when integrated in the observer and in the adaptive law, cause $\hat{\theta}$ to drift to the boundaries of the projection set \mathcal{S}_θ and obstruct convergence. This has been observed in simulations when g_{p1} is too low. Since ϕ is always persistently exciting no further robustifications of the adaptive algorithm are deemed necessary.

7 Observer Scheme 2

Since W_{c1} is an expensive and often imprecise measurement, it is desirable to avoid it. Consequently, the identification scheme can not rely on W_{c1} , which is attainable in any of the coordinates (p_1, m_1) , (p_1, T_1) or (m_1, T_1) by measuring p_1, T_1, T_{ic}, N and using a constant instead of \tilde{W}_{c1} . To remove the errors from this approximation we have to have a closed loop observer. This is possible in all three coordinates since we can construct $\tilde{m}_1 = \frac{1}{k_1^2} \frac{\bar{p}_1}{T_1}$ and use it in the feedback. A closed loop observer will also produce a faster convergence of the estimates only limited by the time constant of the measurements, and is less sensitive to modeling errors.

The observer with state $x^T = [m_1, T_1]^T$ becomes

$$\begin{aligned} \dot{\hat{m}}_1 &= -k_1^2 k_3 N_1 \tilde{m}_1 \mathcal{P}(N) \hat{\theta} + \bar{W}_{c1} \\ &+ g_{m1} \left(\frac{1}{k_1^2} \frac{\bar{p}_1}{T_1} - \hat{m}_1 \right) \end{aligned} \quad (26)$$

$$\begin{aligned} \dot{\hat{T}}_1 &= -(\gamma - 1)k_1^2 k_3 N \bar{T}_1 \mathcal{P}(N) \hat{\theta} + \gamma \frac{1}{\bar{m}_1} \bar{W}_{c1} \bar{T}_{ic} \\ &\quad - \frac{\bar{T}_1}{\bar{m}_1} \bar{W}_{c1} + g_{T1} (\bar{T}_1 - \hat{T}_1) \end{aligned} \quad (27)$$

$$\hat{W}_{1e} = k_1^2 k_3 N \mathcal{P}(N) \hat{m}_1 \hat{\theta}. \quad (28)$$

The adaptive error, $\epsilon(t) = (z - \hat{z})(t)$, becomes

$$\begin{aligned} \epsilon(t) &= (H_{df} \tilde{T}_1)(t) + (H_{df} \tilde{m}_1)(t) \left(H_f \frac{1}{\bar{m}_1} (\bar{T}_1 - \gamma \bar{T}_{ic}) \right) (t) \\ &\quad + g_{m1} (H_f \frac{\tilde{m}_1}{\bar{m}_1} (\bar{T}_1 - \gamma \bar{T}_{ic}))(t) \\ &\quad + g_{T1} (H_f \tilde{T}_1)(t) + \epsilon \end{aligned} \quad (29)$$

where we have neglected the measurement errors $T_1 - \bar{T}_1$, $m_1 - \bar{m}_1$ and $T_{ic} - \bar{T}_{ic}$ and the error, ϵ , from breaking a H_f operator into two terms which is negligible if $\frac{1}{\bar{m}_1} (T_1 - \gamma T_{ic}) - H_f (\frac{1}{\bar{m}_1} (T_1 - \gamma T_{ic}))$ is small. The regressor vector becomes $\phi(N, t) = \gamma k_1^2 k_3 (H_f N \mathcal{P}(N) (\bar{T}_{ic} - \bar{T}_1))(t)$. All signals in (29) are available, and the adaptive law is the same as in scheme one (23) and (24). The five filters (H_f and H_{df}) are implemented as in scheme 1.

Since the regressor, ϕ , is zero in steady state due to the term $T_{ic} - T_1$, ϕ is not always persistently exciting. The adaptive scheme will therefore only converge under non-equilibrium conditions of the engine. In practice this is not a problem since the adaption can be switched off when T_1 is changing slower than some chosen threshold.

Condition 4 $\Delta p_1 = 0$ and $\dot{\bar{T}}_{ic} = 0 \forall t \geq t_0$, and ϕ is persistently exciting of order one

Proposition 2 *The adaptive observer (26)-(28) with the update law (23) and (24) driven by the identification error (29) with the filters implemented as (21) and (22) achieves the following:*

1. Condition 1 implies $\hat{\theta}, x \in \mathcal{L}_\infty$
2. If further Condition 4 is satisfied $\tilde{\eta}_v, \hat{W}_{1e} \rightarrow 0$ exponentially as $t \rightarrow \infty$

For a proof see [9].

This scheme is not vulnerable to the possible errors in the W_{c1} measurement, but T_{ic} must be measured with a moderate bandwidth device with good precision to give an unbiased $\hat{\theta}$, which will not converge faster than the timeconstant of \bar{T}_1 . In addition, the observer equation for \hat{m}_1 (26) is closed loop which gives better robustness to modelling errors, and a more reliable \hat{W}_{1e} estimate. These beneficial features have been traded with one more measurement, a higher computational cost, slower convergence time for $\hat{\theta}$, and a requirement of persistency of excitation of ϕ .

8 Simulations

All simulations have been performed with a mean value model of a turbocharged 2.0 l diesel engine with variable geometry turbocharger and without an intercooler. The fueling level was 5 kg/h, and had a positive step at time 0.2 s to 15 kg/h and a negative step back to 5 kg/h at t=0.7

s. $\bar{p}_1 = H_{p1}(p_1 + \Delta p_1)$, where the time constant of H_{p1} is 5 ms, and $\Delta p_1(t) = (0.127324 - |\sin(\frac{2\pi}{60} N(t))|) 0.0125 p_1$ (2.5% ripple in \bar{p}_1). $\bar{W}_{c1} = H_{wc1} W_{c1}$ with a time constant of 20 ms. The volumetric efficiency of the model was: $[H_f(\tau) \mathcal{P}_m^3(N) (1 - 0.003(p_2' - p_1))](t)$ where $p_2'(t) = p_2(t - \delta(t))$, $\delta(t) = \frac{60}{N(t)} \frac{1}{2}$ (one event) and $H_f(N)$ had a time constant of $\frac{\delta(\tau)}{2}$ (half event).

The pumping rate for the speed density and manifold air flow schemes was $P(N, p_1) = ((\mathcal{P}_m^3(N) + 0.15)(1 - 0.003(p_{2mean} - p_1)))$ where p_{2mean} was taken to be the average value of p_2 in the simulation. The time constant for \bar{T}_1 was 1.0 s in the MAF scheme.

The η_v parameterization in scheme 1 was $\hat{\eta}_v = (\mathcal{P}_m^3(N) + 0.15) \hat{\theta}$, and the simulation parameters were: $k_w = 0.05$, $P(t_r) = 0.0002$, $\Gamma = 0.00004$, $g_{p1} = 1000$, $\bar{T}_{ic} = 200 + 1.04 \bar{p}_1 / p_a$ where $p_a = 101 \text{ kPa}$ in both the simulation model and the observer.

The results for scheme 1 are shown in Figure 3, and illustrates that our method is significantly better in estimating the transient behavior of the air charge W_{1e} . Scheme 2 has a slower W_{1e} estimate than scheme 1, but achieves this without measuring W_{c1} .

References

- [1] L. Guzzella and A. Amstutz, "Control of diesel engines," *IEEE Control Systems Magazine*, vol. 18, no. 2, pp. 53–71, 1998.
- [2] A. Amstutz and L. R. Del Re, "EGO sensor based robust output control of EGR in diesel engines," *IEEE Transactions on Control System Technology*, vol. 3, no. 1, 1995.
- [3] S. Diop, P. E. Moral, I. V. Kolmanovsky, and M. V. Nieuwstadt, "Intake oxygen concentration estimation for DI diesel engines," *Proceedings of the 1999 IEEE International Conference on Control Applications*, vol. 1, pp. 852–7, 1999.
- [4] J. B. Heywood, *Internal Combustion Engine Fundamentals*. New York: McGraw-Hill, 1988.
- [5] J. W. Grizzle, J. A. Cook, and W. P. Milam, "Improved cylinder air charge estimation for transient air fuel ratio control," *Proceedings of the 1994 American Control Conference*, vol. 2, pp. 1568–73, 1994.
- [6] W. W. Yuen and H. Servati, "A mathematical engine model including the effect of engine emissions," SAE Technical Paper Series 840036, 1984.
- [7] C. F. Taylor, *The Internal-Combustion Engine in Theory and Practice*. Cambridge, Massachusetts: M.I.T. Press, 2. ed., 1985.
- [8] R. Hermann and A. J. Krener, "Nonlinear controllability and observability," *IEEE Trans. on Automatic Control*, vol. 22, pp. 728–740, 1977.
- [9] O. F. Storset, "Air charge estimation for turbocharged diesel engines," Master's thesis, University of California Santa Barbara, 2000.
- [10] I. Watson and M. S. Janota, *Turbocharging the Internal Combustion Engine*. New York: Wiley, 1982.
- [11] P. A. Ioannou and J. Sun, *Robust Adaptive Control*. New Jersey: Prentice Hall, 1996.